Fission fragment angular distributions for ^{11}B and ^{19}F+^{238}U systems

A. Karnik, S. Kailas, A. Chatterjee, A. Navin, A. Shrivastava, P. Singh, and M. S. Samant*
Nuclear Physics Division, Bhabha Atomic Research Centre, Bombay 400 085, India
(Received 6 June 1995)

The fission fragment angular distributions were measured at energies above the fusion barrier, for the systems ^{11}B and ^{19}F + ^{238}U. An analysis of the present data along with those already available for the systems ^{6,7}Li, ^{12}C, and ^{16}O + ^{238}U was made in terms of the saddle-point statistical model. While the anisotropies were "normal" for ^{6,7}Li, ^{11}B, ^{12}C+^{238}U systems, the ones for ^{16}O and ^{19}F+^{238}U systems were found to be "anomalous." The entrance channel mass asymmetry dependence of the anisotropies as observed here is consistent with the expectations of preequilibrium fission dynamics. This result emphasizes the importance of preequilibrium fission in heavy-ion induced fusion-fission reactions.

PACS number(s): 25.70.Jj

I. INTRODUCTION

In many investigations of heavy-ion induced fusion-fission reactions, the measured fission fragment anisotropies are significantly larger than the predictions of the standard saddle-point statistical model (SSPSM) [1–10]. It appears that these anomalous anisotropies are a manifestation of the various reaction dynamics in different energy regions. There are two distinct energy regions, (i) above the fusion barrier (V_B) and (ii) near and below the barrier. At above barrier energies, the preequilibrium (PE) fission [4] contribution to the total fission cross section becomes very important. The characteristic signature of PE fission is an entrance channel dependence of the fission fragment anisotropies. At energies well above the barrier, it was observed [11,12] that for the systems ^{9}Be, ^{10}B, ^{12}C + ^{232}Th, and ^{237}Np, the experimental angular distributions follow the predictions of the SSPSM, whereas the anisotropies are anomalously large for the heavier projectiles like ^{16}O and ^{19}F. This was taken as an evidence of PE fission. However, not enough data exist for the systems ^{16}O, ^{19}F + ^{232}Th, and ^{237}Np at energies well above the barrier. At near-barrier energies, the reason for large anisotropies observed in the case of ^{12}C + ^{232}Th [13,14], ^{12}C + ^{237}Np [11,15], and ^{11}B + ^{238}U [15,16] systems may be due to couplings of the other degrees of freedom to the entrance channel. It is seen [13–16] that, even for these systems where the PE fission contribution is not expected, the barrier dependent effects are present, independent of the entrance channel.

If measurements are made at energies well above the fusion barrier, the barrier dependent effects can be neglected and the effect of entrance channel dependence, if present, can be studied unambiguously. To investigate the role of PE fission in heavy-ion induced fusion-fission reactions, we have carried out measurements of fission fragment (FF) anisotropies for the systems ^{11}B and ^{19}F + ^{238}U, from near-barrier to above barrier energies. The FF anisotropy data for ^{11}B + ^{238}U reported here extend the work of Zhang *et al.* [15] to energies well above the fusion barrier. In addition, fission excitation function and angular distribution data are available for the ^{6,7}Li [17], ^{11}B [15,18], ^{12}C [18–20], and ^{16}O [2,18,20–24] + ^{238}U systems over a range of energies. Combining these data along with the present measurements, we have investigated the entrance channel dependence of the fission fragment anisotropies in ^{238}U + projectile systems.

II. EXPERIMENTAL DETAILS AND DATA ANALYSIS

The experiment was performed using ^{11}B and ^{19}F beams from the BARC-TIFR 14UD Pelletron accelerator at Bombay. The beam energies used were 57.6, 61.6, 65.7, and 69.7 MeV for ^{11}B and 103.6, 107.6, 111.7, and 114.7 MeV for ^{19}F. A $\sim$250 μg/cm^2 thick ^{nat}U target was prepared by electrodeposition on a 400 μg/cm^2 rolled Al foil. The experimental setup consisting of three ΔE-E surface barrier and three gas-Si telescopes used for the detection of fission fragments is shown in Fig. 1. For the surface barrier telescopes most of the fission fragments were stopped in the ΔE detector (12 μm) and those which reached the E detector (1 mm) were well separated in energy from the scattered elastic, inelastic, and transfer particles. The gas-Si telescopes consisted of a common ΔE gas ionization detector backed by three discrete E-Si detectors (2 mm). The gas detector was trapezoidal in shape with two parallel electrodes separated by a distance of 84 mm. Between the two electrodes a Frisch grid was positioned at a distance of 12 mm from the anode. The

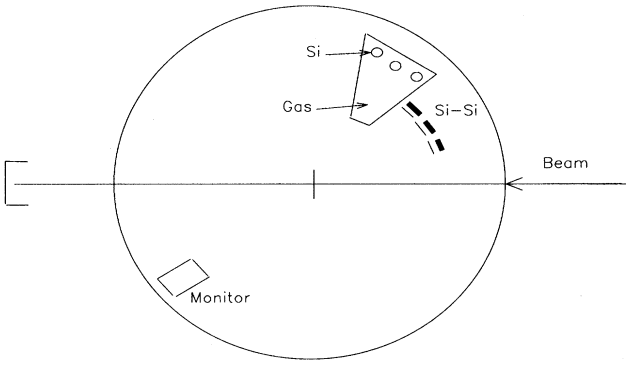

FIG. 1. Experimental setup showing the detector configuration.

*Present address: Tata Institute of Fundamental Research, Bombay 400 005, India.

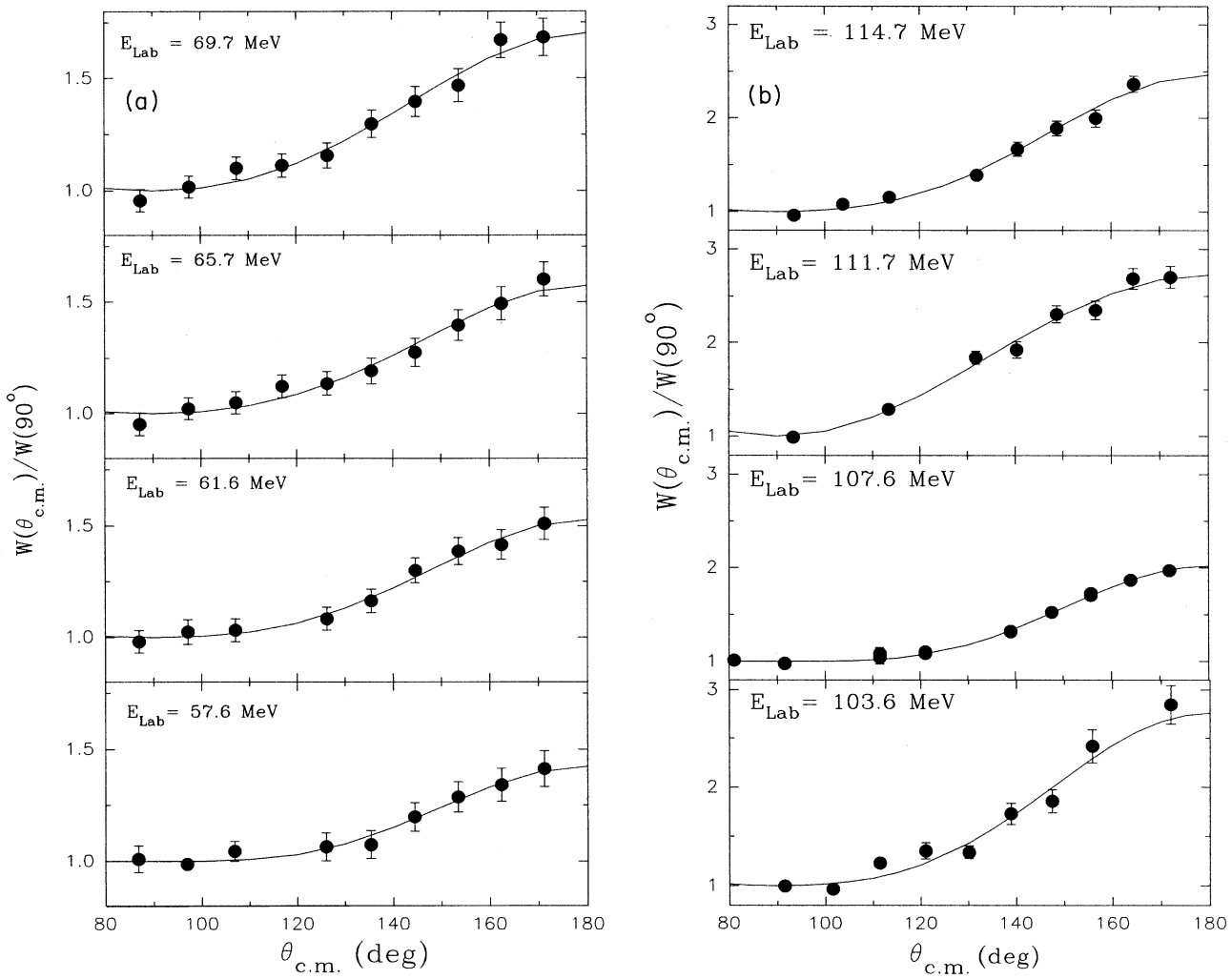

FIG. 2. (a) Fission fragment angular distributions for the system $^{11}B + ^{238}U$. The solid lines are Legendre polynomial fits to the data. (b) Same as (a) for the $^{19}F + ^{238}U$ system.

active gas length for ΔE was 200 mm. P-10 gas at a low pressure of 10 mbar was maintained in the flow mode so as to obtain a good separation between fission and projectilelike particles, in the ΔE(gas)-E(Si) spectrum. The anode and Frisch grid were kept at 270 and 150 V, respectively, with reference to the cathode which was grounded. The E(Si) detectors were mounted inside the ionization detector in an arc shaped housing with a separation of 10° at a distance of 20 cm from the entrance window. A surface barrier monitor detector of 300 μm thickness was kept at 40° with respect to the beam, to detect the elastically scattered particles.

The data were collected as two dimensional spectra for each of the six telescopes deriving the trigger signals from the ΔE detectors in the case of the surface barrier telescopes and from the E detectors in the case of the gas-surface barrier hybrid telescopes. Fission spectra were obtained by appropriate projections on ΔE in all the cases. The angular distributions of fission fragments were measured in the range of 80° to 170° in the laboratory. The relative solid angles between the different detectors were determined by taking data at overlapping angles. The absolute cross sections were extracted by normalizing the fission yields to the monitor yields, assuming the latter to arise from Rutherford scattering. The fission fragment angular distributions were transformed to the center-of-mass system assuming symmetric mass division and using Viola's systematics [25]. The angular distributions $W(\theta)$ were fitted to a sum of Legendre polynomials to extract the fission fragment anisotropies, $A = W(180°)/W(90°)$. The data and the fits for ^{11}B and ^{19}F at different energies are shown in Figs. 2(a) and 2(b). The errors on the fission cross sections and the anisotropies are due to counting statistics and interdetector solid angle normalizations. The fission excitation functions for these systems are shown in Figs. 3(a) and 3(b). The fission fragment anisotropies for the above systems as well as for $^{6,7}Li$, ^{12}C, and $^{16}O + ^{238}U$ are shown in Fig. 4.

III. CALCULATIONS

The FF anisotropy is given as

$$A \simeq 1 + \frac{\langle I^2 \rangle}{4K_0^2} \tag{1}$$

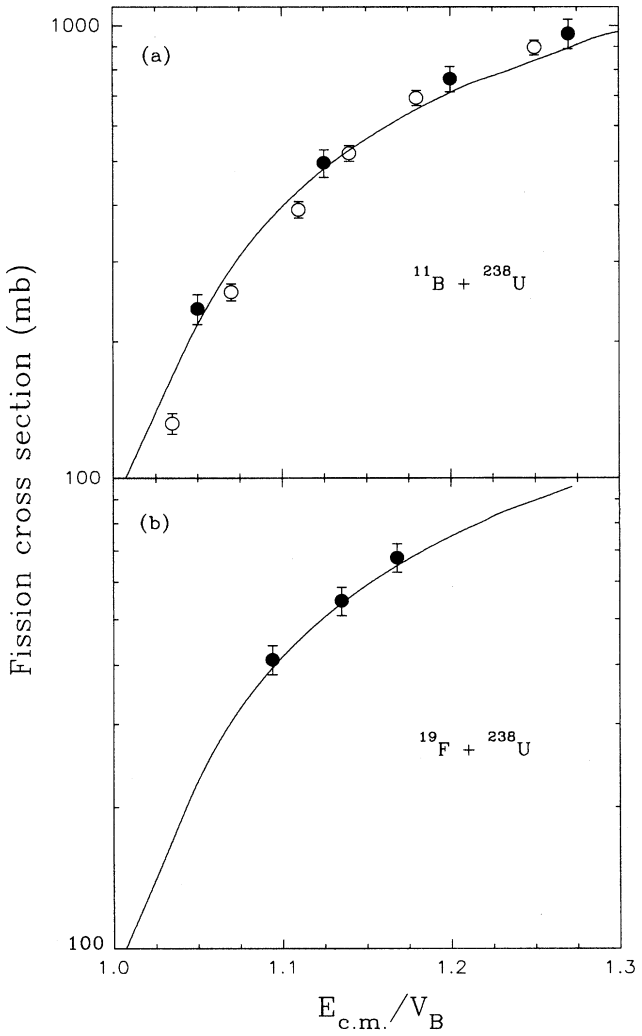

FIG. 3. Fission cross sections as a function of $E_{c.m.}/V_B$ for (a) ^{11}B + ^{238}U and (b) ^{19}F + ^{238}U systems. The filled circles are the present measurements, open circles are from Ref. [18], and the solid lines are Wong model calculations.

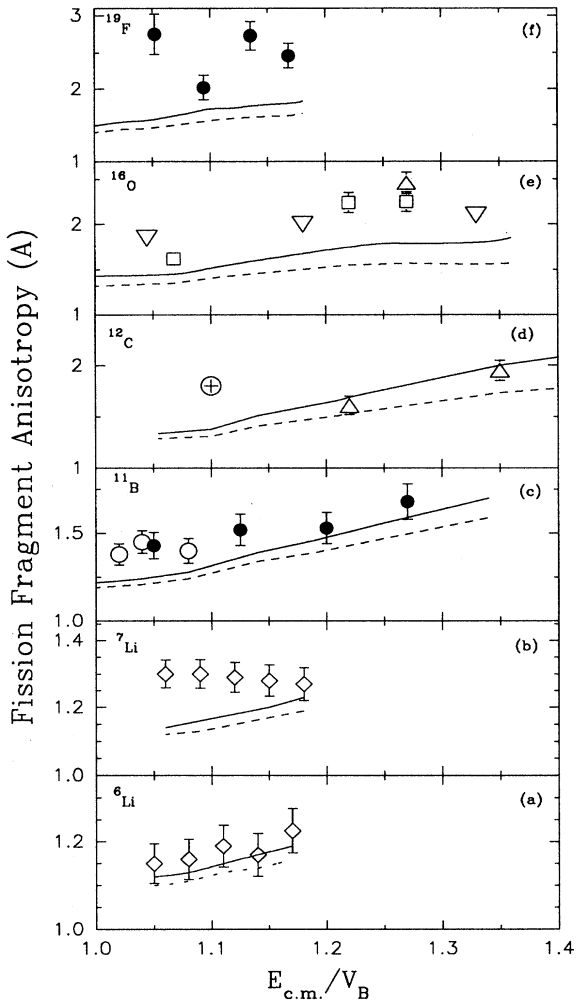

FIG. 4. Experimental and SSPSM predicted anisotropies as a function of $E_{c.m.}/V_B$ for the systems ^{6,7}Li, ^{11}B, ^{12}C, ^{16}O, ^{19}F + ^{238}U. The anisotropy calculations for $a=A_{CN}/8$ MeV^{-1} with prescission neutron correction (ν_{ssc} = 0) are shown by the solid lines; the dashed lines are without prescission neutron correction. The data are from the present work, (solid circles), Ref. [15], (open circles), Ref. [17], (open diamonds), Ref. [19], (star), Ref. [20], (open triangles), Ref. [24], (open inverted triangles), and Refs. [2,22,23], (open squares).

where K_0^2 is the variance of K (projection of the total angular momentum I on the symmetry axis of the fissioning system) distribution and $\langle l^2 \rangle$ is the mean square spin of the compound nucleus. The experimental fission excitation functions were fitted using the Wong model [26] to obtain the required $\langle l^2 \rangle$ values. The $\langle l^2 \rangle$ values calculated using the zero point model of Esbensen [27] are typically 10% higher than those obtained from the Wong model. The deformation parameter of the ^{238}U target nucleus was taken as β_2 = 0.28. The Wong model fits to the measured fission excitation functions are shown in Fig. 3. K_0^2 is given by

$$K_o^2 = \frac{J_{\text{eff}}}{\hbar^2} T \tag{2}$$

where J_{eff} is the effective moment of inertia of the compound nucleus, T is the nuclear temperature given by $\sqrt{E^*/a}$, E^* is the excitation energy, and a is the level density parameter of the compound nucleus at the saddle point. In the present calculations we have taken $a=A_{CN}/8$ MeV^{-1}.

The excitation energy E^* at the saddle point is calculated using the relation

$$E^* = E_{c.m.} + Q - B_f(\langle l^2 \rangle) - E_{\text{rot}}(\langle l^2 \rangle) - E_n \text{ MeV} \tag{3}$$

where Q is the Q value for the formation of the compound nucleus. The spin dependent fission barrier $B_f(\langle l^2 \rangle)$, ground state rotational energy $E_{\text{rot}}(\langle l^2 \rangle)$, and effective moment of inertia $J_{\text{eff}}(\langle l^2 \rangle)$ are calculated using the Sierk model [28] and the sharp cutoff approximation for the spin distribution. The dependence of B_f, E_{rot}, and J_{eff} on $\langle l^2 \rangle$ for the system ^{16}O + ^{238}U was parametrized as given below:

$$B_f(\langle l^2\rangle) = -0.0013\langle l^2\rangle + 1.52 \text{ MeV}, \quad (4)$$

$$E_{\text{rot}}(\langle l^2\rangle) = 0.0065\langle l^2\rangle - 0.017 \text{ MeV}, \quad (5)$$

$$\frac{J_{\text{eff}}}{\hbar^2}(\langle l^2\rangle) = 0.14\langle l^2\rangle + 200 \text{ MeV}^{-1}. \quad (6)$$

In Eq. (3), E_n, the average energy removed by the evaporated neutrons from the compound nucleus, is taken as

$$E_n = \nu_{\text{pre}}(B_n + 2T) \text{ MeV}, \quad (7)$$

where ν_{pre} is the prescission neutron multiplicity, B_n is the neutron binding energy, and $2T$ gives the average kinetic energy of the evaporated neutrons. Experimentally, it is observed that the number of particles emitted prior to fission is more than that predicted by the usual statistical model. Therefore ν_{pre} was calculated using the systematics of Newton [29] for heavy-ion induced fission reactions. The dependence of ν_{pre} on excitation energy can be expressed as

$$\nu_{\text{pre}}(E_x) = 0.077E_x - 1.75 \quad (8)$$

where $E_x = E_{\text{c.m.}} + Q$. The effect of neutron evaporation prior to reaching the saddle point is to reduce the temperature of the fissioning nucleus which in turn increases the FF anisotropy. Due to prescission neutron evaporation, the spin distribution is also affected though not significantly. Prescission neutrons (ν_{pre})can be emitted before the saddle point (ν_d) or between saddle and scission (ν_{ssc}). Only ν_d influences the fission angular distribution. Assuming all the prescission neutrons are emitted before the saddle point, upper limits of the SSPSM anisotropies have been calculated (indicated as $\nu_{\text{ssc}} = 0$ in Figs. 4 and 5). A calculation has also been carried out taking into account ν_d and ν_{ssc} components. The multiplicity of presaddle neutrons, ν_d, was estimated from the systematics of Saxena *et al.* [30] and this has been used to calculate the anisotropies (indicated as $\nu_{\text{ssc}} > 0$ in Fig. 5). A comparison of the two calculations ($\nu_{\text{ssc}} = 0$ and $\nu_{\text{ssc}} > 0$) with the data for the ^{16}O + ^{238}U system is shown in Fig. 5. In the same figure, the sensitivity of the calculations to the level density parameter a for $a = A_{\text{CN}}/8$ MeV^{-1} and $a = A_{\text{CN}}/10$ MeV^{-1} is also shown.

IV. RESULTS AND DISCUSSION

In our measurements, we have not distinguished compound nuclear fission (CNF) events from the incomplete momentum transfer events. For energies much above the fusion barrier, transfer induced fission is not a significant fraction of the total fission. Also, in the measurements where compound nuclear fission events have been separated, the CNF anisotropies are found to be higher than the total fission anisotropies [31,32].

The measured anisotropies for various systems as a function of $E_{\text{c.m.}}/V_B$ are shown in Fig. 4. The dashed lines are the SSPSM predictions without the corrections for prescission neutron emission. The solid lines are SSPSM calculations with the ν_{pre} correction taking $\nu_{\text{ssc}} = 0$. The prescission neutron correction becomes important at higher energies [7,12],

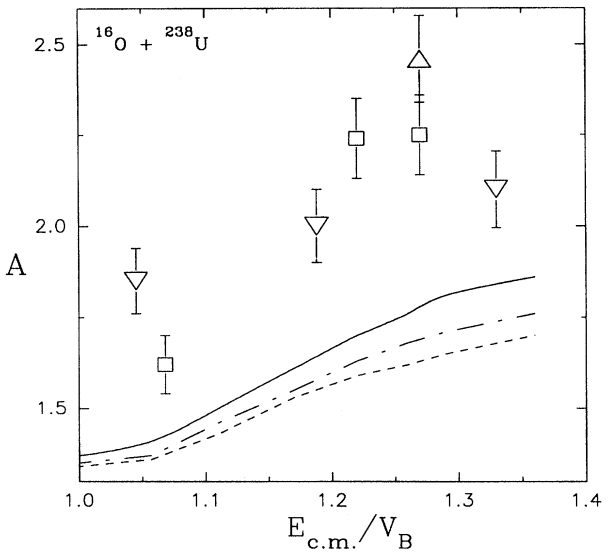

FIG. 5. Experimental and SSPSM predicted anisotropies as a function of $E_{\text{c.m.}}/V_B$ for the system ^{16}O + ^{238}U. The anisotropy calculations with prescission neutron corrections (see text) are shown by solid line for $a = A_{\text{CN}}/8$ MeV^{-1} ($\nu_{\text{ssc}} = 0$), the dot-dashed line for $a = A_{\text{CN}}/8$ MeV^{-1} ($\nu_{\text{ssc}} > 0$), and the short-dashed line for $a = A_{\text{CN}}/10$ MeV^{-1} ($\nu_{\text{ssc}} = 0$). The data are from Ref. [20], (open triangles), Ref. [24], (open inverted triangles), and Refs. [2,22,23], (open squares).

where it can give about 10–12 % higher values for the anisotropies compared to the first chance fission anisotropies. While the ^{6}Li data are described very well over the entire energy range, the ^{7}Li, ^{11}B, and ^{12}C data are consistent with the calculations only for $E_{\text{c.m.}}/V_B \geq 1.15$. However, the anisotropies for projectiles like ^{16}O and ^{19}F are considerably higher than the theoretical predictions in the same energy region.

In this discussion we consider only the energy range $1.15 \leq E_{\text{c.m.}}/V_B \leq 1.3$. In this energy range $B_f \sim T$ and hence the PE fission mechanism is expected to be observed unambiguously. The lower limit is due to channel coupling effects which are dominant at near-barrier energies. The upper limit has been chosen to ensure that other processes like fast fission, which are important beyond this energy range, are not included. The limiting energies mentioned above are typical and it is this energy region which is likely to favor the occurrence of the PE process. In Fig. 6, we have plotted values of $(A_{\text{exp}}-1)/(A_{\text{th}}-1)$ for different systems as a function of mass asymmetry, $\alpha = (A_T - A_P)/(A_T + A_P)$. For the sake of clarity in the figure, representative values of $(A_{\text{exp}}-1)/(A_{\text{th}}-1)$ averaged over the energy region mentioned have been plotted for each case. The hatched area in the figure represents the Businaro-Gallone (BG) critical mass asymmetry region [33] taking into consideration the variation of α_{BG} with fissility for the various systems. For $\alpha > \alpha_{\text{BG}}$ the anisotropies can be explained by the SSPSM, whereas they are anomalously large for $\alpha < \alpha_{\text{BG}}$. The existence of this kind of entrance channel dependence of anisotropies across the BG boundary is a signature for the presence of PE fission in the latter and its absence in the former.

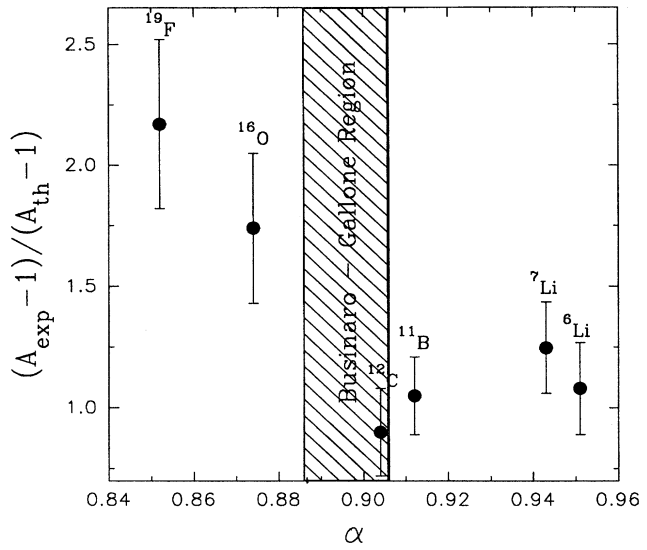

FIG. 6. Values of $(A_{exp}-1)/(A_{th}-1)$ are plotted as a function of the entrance channel mass asymmetry parameter α for the systems ^{6,7}Li, ^{11}B, ^{12}C, ^{16}O, ^{19}F + ^{238}U. The shaded region represents the α_{BG} range for the various systems.

V. SUMMARY

We have reported measurements of fission fragment angular distributions for ^{11}B, ^{19}F + ^{238}U systems extending from near-barrier to well above barrier energies. The data for ^{11}B + ^{238}U are an extension to higher energies of measurements of Zhang *et al.* [15]. In this system the anisotropy values are anomalous at near-barrier energies and are normal at higher energies. At energies well above the barrier, the fission fragment anisotropies for projectiles from ^{6}Li to ^{12}C can be described by the SSPSM. However as the projectiles become heavier (^{16}O, ^{19}F), the anisotropy values do not follow the SSPSM predictions. This kind of entrance channel dependence of fission fragment anisotropies is similar to the one observed earlier in Th and Np systems. In the energy region $E_{c.m.}/V_B \sim$ 1.15–1.3, an entrance channel dependence of anisotropies is clearly seen and this is a characteristic of preequilibrium fission.

ACKNOWLEDGMENTS

The authors thank Dr. S. S. Kapoor for his keen interest in this work and useful discussions. We also thank the pelletron staff for the efficient operation of the machine and Dr. R. J. Singh for preparing the ^{238}U targets. One of us (A.K.) would like to thank the Department of Atomic Energy and Board of Research in Nuclear Sciences for financial support to carry out this research work.

[1] L. C. Vaz and J. M. Alexander, Phys. Rep. **97**, 1 (1983).
[2] B. B. Back, R. R. Betts, J. E. Ginder, B. D. Wilkins, S. Saini, M. B. Tsang, C. K. Gelbke, W. G. Lynch, M. A. McMahan, and P. A. Baisden. Phys. Rev. C **32**, 195 (1985) .
[3] R. Freifelder, M. Prakash, and J. M. Alexander, Phys. Rep. **133**, 315 (1986).
[4] V. S. Ramamurthy and S. S. Kapoor, Phys. Rev. Lett. **54**, 178 (1985); in *Proceedings of the International Conference on Nuclear Physics*, Harrogate, U.K., 1986, edited by J. L. Durell, J. M. Irvine, and G. C. Morrison, IOP Conf. Proc. No. 86 (Institute of Physics, Bristol, 1986), Vol. 1, p. 292.
[5] R. Vandenbosch, T. Murakami, C. C. Sahm, D. D. Leach, A. Ray, and M. J. Murphy, Phys. Rev. Lett. **56**, 1234 (1986).
[6] T. Murakami, C. C. Sahm, R. Vandenbosch, D. D. Leach, A. Ray, and M. J. Murphy, Phys. Rev. C **34**, 1353 (1986).
[7] H. H. Rossner, J. R. Huizenga, and W. U. Schröder, Phys. Rev. C **33**, 139 (1986).
[8] C. Ngô, Prog. Part. Nucl. Phys. **16**, 139 (1986).
[9] J. M. Alexander, Ann. Phys. (Paris) **12**, 603 (1987).
[10] J. O. Newton, Sov. J. Nucl. Phys. **21**, 349 (1990).
[11] V. S. Ramamurthy, S. S. Kapoor, R. K. Choudhury, A. Saxena, D. M. Nadkarni, A. K. Mohanty, B. K. Nayak, S. V. S. Sastry, S. Kailas, A. Chatterjee, P. Singh, and A. Navin, Phys. Rev. Lett. **65**, 25 (1990).
[12] A. Saxena, S. Kailas, A. Karnik, and S. S. Kapoor, Phys. Rev. C **47**, 403 (1993).
[13] A. Karnik, S. Kailas, A. Chatterjee, P. Singh, A. Navin, D. C. Biswas, D. M. Nadkarni, A. Shrivastava, and S. S. Kapoor, Z. Phys. A **351**, 195 (1995).
[14] N. Majumdar, P. Basu, M. L. Chatterjee, P. Bhattacharya, D. C. Biswas, A. Saxena, R. K. Choudhury, and D. M. Nadkarni, Symp. Nucl. Phys. (India) **36B**, 196 (1993).
[15] H. Zhang, Z. Liu, J. Xu, X. Qian, S. Chen, and L. Lu, Phys. Rev. C **47**, 1309 (1993).
[16] A. Karnik, S. Kailas, A. Chatterjee, A. Navin, A. Shrivastava, P. Singh, M. S. Samant, and S. S. Kapoor, in *Workshop on heavy ion fusion, Exploring the variety of nuclear properties*, Padova, Italy, 1994, edited by A. M. Stefanini, G. Nebbia, S. Lunardi, G. Montagnoli, and A. Vitturi (World Scientific, Singapore, 1994), p. 350.
[17] H. Freiesleben, G. T. Rizzo, and J. R. Huizenga, Phys. Rev. C **12**, 42 (1975).
[18] V. E. Viola and T. Sikkeland, Phys. Rev. **128**, 767 (1962).
[19] T. Sikkeland, Phys. Rev. **123**, 2112 (1961).
[20] S. A. Karamyan, I. V. Kuznetsov, T. A. Muzychka, Yu. Ts. Oganesyan, Yu. E. Penionzhkevich, and B. I. Pustylnik, Sov. J. Nucl. Phys. **6**, 360 (1968); S. A. Karamyan, V. N. Bugrov, and N. I. Spiridonov, *ibid.* **43**, 339 (1986).
[21] H. Zhang, Z. Liu, J. Xu, X. Qian, Y. Qiao, C. Lin, and K. Xu, Phys. Rev. C **49**, 926 (1994).
[22] A. Gavron, P. Eskola, A. J. Sierk, J. Boissevain, H. C. Britt, K. Eskola, M. M. Fowler, H. Ohm, J. B. Wilhelmy, S. Wald, and R. L. Ferguson, Phys. Rev. Lett. **52**, 589 (1984).
[23] J. Tõke, R. Bock, Dai Guang-Xi, A. Gobbi, S. Gralla, K. D.

Hildenbrand, J. Kuzminski, W. F. J. Müller, A. Olmi, W. Reisdorf, S. Bjornholm, and B. B. Back, Phys. Lett. **142B**, 258 (1984).
[24] W. Q. Shen, J. Albinski, A. Gobbi, S. Gralla, K. D. Hildenbrand, N. Herrmann, J. Kuzminski, W. F. J. Müller, H. Stelzer, J. Tõke, B. B. Back, S. Bjornholm, and S. P. Sorensen, Phys. Rev. C **36**, 115 (1987).
[25] V. E. Viola, K. Kwiatkowski, and M. Walker, Phys. Rev. C **31**, 1550 (1985).
[26] C. Y. Wong, Phys. Rev. Lett. **31**, 766 (1973).
[27] H. Esbensen, Nucl. Phys. **A352**, 147 (1981).
[28] A. J. Sierk, Phys. Rev. C **33**, 2039 (1986).
[29] J. O. Newton, Pramana. J. Phys. **39**, 175 (1989).
[30] A. Saxena, A. Chatterjee, R. K. Choudhury, S. S. Kapoor, and D. M. Nadkarni, Phys. Rev. C **49**, 932 (1994).
[31] N. Majumdar, P. Bhattacharya, D. C. Biswas, R. K. Choudhury, D. M. Nadkarni, and A. Saxena, Phys. Rev. C **51**, 3109 (1995).
[32] D. J. Hinde, M. Dasgupta, J. R. Leigh, J. P. Lestone, J. C. Mein, C. R. Morton, J. O. Newton, and H. Timmers, Phys. Rev. Lett. **74**, 1295 (1995).
[33] U. L. Businaro and S. Gallone, Nuovo Cimento **5**, 315 (1957).